

# Performance of the LiF-TEA Ring Imaging Cherenkov Detector at CLEO

R. Sia<sup>\*</sup>

*Department of Physics, Syracuse University, Syracuse, New York 13244*  
*E-mail: rsia@phy.syr.edu*

---

## Abstract

We describe the particle identification capability of the CLEO RICH system. This system consists of a 1 cm thick LiF radiator coupled to a photon detector that uses wire proportional chambers filled with a mixture of CH<sub>4</sub> and TEA. We discuss the yield of photoelectrons observed per ring and the angular resolution. We show the efficiencies achieved for particle identification and the associated fake rates from data collected with both CLEO III and CLEO-c detectors. Finally we show examples of the particle separation ability which is excellent for both CLEO III and CLEO-c data.

---

## 1 Introduction

In 1999 a particle identification system based on Ring Imaging Cherenkov detector (RICH) technology, a new vertex detector and a new wire drift chamber were added to the CLEO detector to probe physics of the decays of  $b$  and  $c$  quarks,  $\tau$  leptons and  $\Upsilon$  mesons produced near 10 GeV in  $e^+e^-$  collisions [1]. With RICH, the goal was to achieve a

$\pi/K$  separation greater than  $4\sigma$  up to 2.65 GeV/c, the mean momentum for pions from  $B \rightarrow \pi\pi$  decays. At this momentum, the Cherenkov angle between  $\pi$  and  $K$  in LiF differs by 14.3 mrad. We expect to have in a 1 cm thick sample at this momentum about 12 detected photons with a resolution per photon of 14 mrad yielding to an angular resolution per track of 4 mrad. This resolution is enough for more than  $3\sigma$  separation in addition to the  $2\sigma$  separation provided by dE/dx information in the drift chamber for momenta higher than 2.2 GeV/c. In this paper, we compare these expectations with the physics performance of the detector that has been used for more than 4 years in CLEO III and recently in CLEO-c at lower center-of-mass

---

<sup>\*</sup> For the CLEO RICH group: M. Artuso, R. Ayad, K. Bukin, A. Efimov, C. Boulahouache, E. Dambasuren, S. Kopp, R. Mountain, G. Majumder, S. Schuh, T. Skwarnicki, S. Stone, G. Viehhauser, J.C. Wang, T. Coan, V. Fadeyev, I. Volobouev, J. Ye, S. Anderson, Y. Kubota, A. Smith.

energies.

## 2 Detector Description

Cherenkov photons are produced in a shell of 1 cm thick LiF crystal radiators which, up to a  $22^\circ$  angle from the center of the solenoid, are sawtooth radiators [2] and the rest planar. The sawtooth radiators are used to prevent total internal reflection of Cherenkov photons where charged particles cross the detector at near normal incidence. The photons then enter a 15.6 cm thick expansion volume filled with pure  $N_2$  gas, as shown in Fig. 1, and get detected in multiwire proportional chambers. The chambers have  $CaF_2$  windows

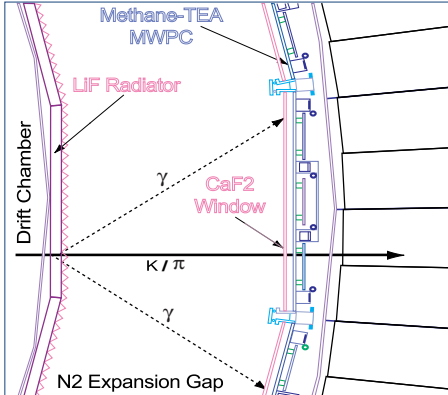


Fig. 1. Sketch of the Cherenkov photon process in the CLEO RICH Detector

and are filled with TEA dispersed in methane that has the ability to detect vacuum ultraviolet photons. Charge signals induced on an array of 230,400 7.5 mm x 8 mm cathode pads are used to measure the position of the Cherenkov photons using custom made low noise and high dy-

namic range VA\_RICH ASIC's that convert the charge signals into differential current signals in order to minimize cross talk in the cables connecting the front end electronics to the data boards. The back end electronics include transimpedance receivers that transform the current signals into voltage signals which get digitized afterwards by 12-bit differential ADC's in the data boards located in the VME crates. More details can be found in [3] and [4].

## 3 PHYSICS PERFORMANCE

### 3.1 Photon Resolution and Photon Yield

The physics performance studies were made previously [3] using either Bhabha or hadronic events<sup>1</sup> where the single photon resolution parameter  $\sigma_\theta$  is the RMS width of the difference between the measured and the expected single-photon Cherenkov angle distribution. The photon yield per track is extracted from the fitted and background subtracted photon yield per track distribution. Consequently, the Cherenkov angle per track is found as the arithmetic mean of all photoelectrons in an image within  $\pm 3\sigma$  for each hypothesis. A summary of the averaged values of

<sup>1</sup> Here, photons that match the most likely mass hypothesis within  $\pm 3\sigma$  were removed from consideration for the other tracks to resolve overlaps between Cherenkov images for different tracks.

Table 1

The averaged values of the single-photon resolution( $\sigma_\theta$ ), the photon yield( $N_\gamma$ ) and the Cherenkov angle resolutions per track( $\sigma_{track}$ ) from Bhabha and hadronic CLEO III events, for flat and sawtooth radiators.

Event Type	Type of Radiators	$\sigma_\theta$ (mrad)	$N_\gamma$	$\sigma_{track}$ (mrad)
Bhabha	planar	14.7	10.6	4.7
	sawtooth	12.2	11.9	3.6
Hadronic	planar	15.1	9.6	4.9
	sawtooth	13.2	11.8	3.7

these parameters for flat and sawtooth radiators are shown in Table 1.

The components of the Cherenkov angular resolution per track are compared with the data as shown in Fig. 2. The resolution is mainly dominated by the chromatic dispersion and the error on the photon emission point. Smaller components include the error on the reconstructed photon position and the error on the charged track’s direction and position determination.

### 3.2 Particle ID Likelihood: Definition and Operating Modes

The particle identification criteria we are using for CLEO III and CLEO-c analysis is different from what we presented in the last section where only the optical path with the closest Cherenkov angle to the expected one was considered. Here, the information on the value of the Cherenkov angle and the photon yield for each hypothesis is translated into a Likelihood of a given photon being due to a particular particle. Contributions

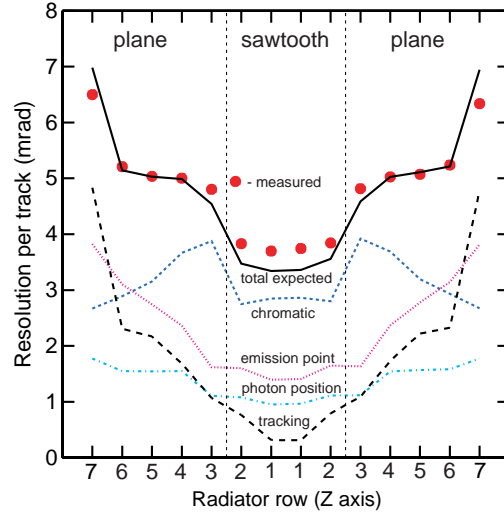


Fig. 2. Cherenkov angle resolution per track versus radiator ring for Bhabha events from data (solid points) and from the sum (solid line) of the different predicted components (as labelled).

from all photons<sup>2</sup> associated with a particular track are weighted by their optical probabilities<sup>3</sup> then summed to form an overall Likelihood denoted as  $L_h$  for each particle hypothesis “ $h$ ” ( $e, \mu, \pi, K$  or  $p$ ), details about the analytical form of the Likelihood function can be found in [3].

<sup>2</sup> with a loose cut-off of  $\pm 5\sigma$ .

<sup>3</sup> which include length of the radiation path and the refraction probabilities.

The CLEO III data at  $e^+e^-$  center-of-mass energies around 10 GeV have been used to evaluate the RICH performance. Since the charge of the slow pion in the  $D^{*+} \rightarrow \pi^+ D^0$  decay is opposite to the kaon charge in the subsequent  $D^0 \rightarrow K^- \pi^+$  decay, the kaon and pion in the  $D^0$  decay can be identified without the RICH information. The efficiencies and fake rates are hence extracted by studying the RICH identification selectivity on the particle species selected with the  $D^*$  tag. Here the  $D^0$  mass peak in the  $K^- \pi^+$  mass distribution is fitted to obtain the number of signal events for each momentum interval. Fig. 3 shows the distribution of  $2 \ln(L_\pi/L_K)$ , which is equivalent to the  $\chi^2$  difference in the Gaussian approximation, for the identified kaons and pions with 1.0 – 1.5 GeV/c momentum.

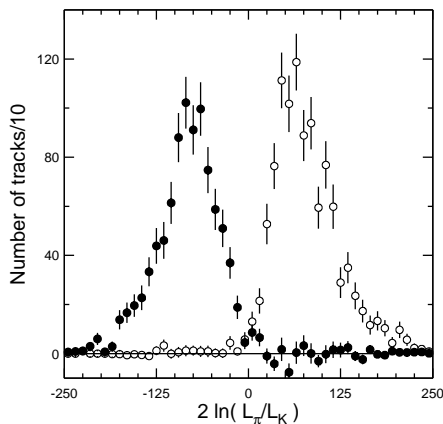


Fig. 3. Distribution of  $2 \ln(L_\pi/L_K) \sim \chi_K^2 - \chi_\pi^2$  for 1.0 – 1.5 GeV/c kaons (filled) and pions (open) identified with the  $D^*$  method.

The detected fraction of kaons (pions) as a function of the cut on

$2 \ln(L_\pi/L_K)$  is shown in Fig. 4 and the pion fake rate for different

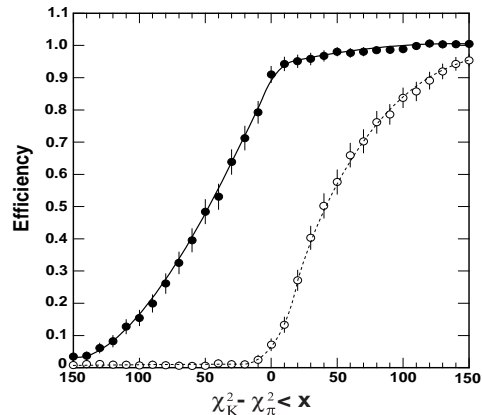


Fig. 4. Kaon efficiency (filled points) and pion fake rate (hollow points) vs various cuts on the  $\chi_K^2 - \chi_\pi^2$  for tracks with 0.7 – 2.7 GeV/c momentum.

kaon efficiencies versus momentum is shown in Fig. 5. Below  $\sim 0.6$  GeV,

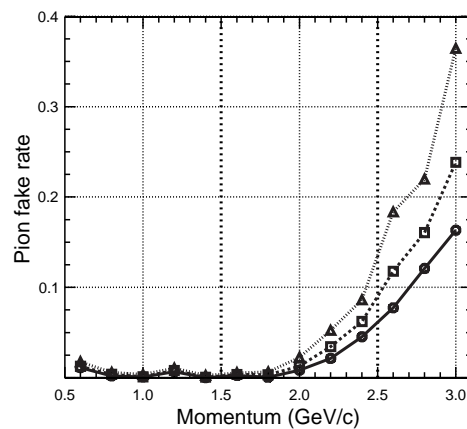


Fig. 5. Pion fake rate vs momentum for different kaon efficiencies: 80% (in circles), 85% (in squares) and 90% (in triangles).

the RICH can be used in the threshold mode. Fig. 6 shows the fraction of kaons (pions) passing the cut restricting the number of photons assigned to the pion hypothesis for tracks near and below the Cherenkov radiation threshold for kaons (0.44 GeV/c).

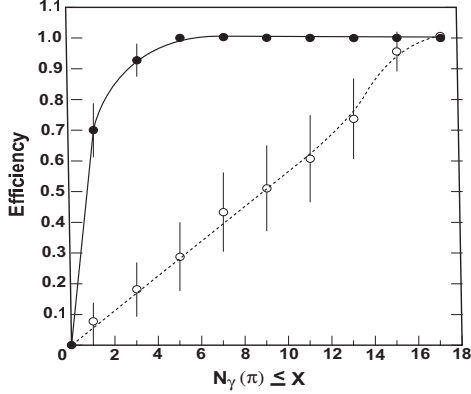


Fig. 6. Kaon efficiency (filled circles) and pion fake rate (empty circles) measured for various cuts on the number of photons assigned to pion hypothesis for tracks with  $|p| < 0.6$  GeV/c.

A summary of pion (kaon) efficiencies and kaon (pion) fake rates from CLEO III data for  $0.9 - 1.5$  GeV/c momentum range with a  $\chi_K^2 - \chi_\pi^2$  cut at 0 is shown in Table 2.

At lower center-of-mass energies near 4 GeV, the CLEO-c program has started extensive studies of charm meson decays. In these analyses, one of the  $D$ 's is reconstructed through hadronic channels while the other  $\bar{D}$  is used as a signal side for various studies. For  $\pi/K$  ID efficiency measurements pions from  $D^0 \rightarrow K\pi\pi^0$ ,  $D^0 \rightarrow K_s\pi\pi$  and  $D^+ \rightarrow K^-\pi^+\pi^+$  decays and kaons from  $D^0 \rightarrow K\pi\pi^0$  and  $D^+ \rightarrow K^-\pi^+\pi^+$  decays are used. The particle identification efficiency is defined in this case as the ratio of the number of  $D^0$  events that passed the particle ID criteria to the number of  $D^0$  events without any PID. Efficiencies and fake rates for 0.9 GeV/c momentum pions and kaons from the data with a  $\chi_K^2 - \chi_\pi^2$  cut at 0 are summarized at the end of Table 2.

### 3.3 Example of Particle ID Performance

We used recently  $0.42 \text{ fb}^{-1}$  of data taken on the  $\Upsilon(5S)$  resonance,  $6.34 \text{ fb}^{-1}$  of data collected on the  $\Upsilon(4S)$  and  $2.32 \text{ fb}^{-1}$  of data taken in the continuum below the  $\Upsilon(4S)$  with the CLEO III detector to measure the branching fraction  $B(\Upsilon(5S) \rightarrow B_s^{(*)} \bar{B}_s^{(*)})$  [5] which has never been measured before. In this analysis, we reconstructed  $D_s$  mesons through the decay mode:  $D_s \rightarrow \phi\pi$  and  $\phi \rightarrow KK$  where we used the RICH information to identify one of the kaons with a momentum higher than  $0.62$  GeV/c. We show in Fig. 7 for instance the large combinatoric backgrounds, from the  $\Upsilon(4S)$  on resonance data mentioned above, that we would have included in the  $D_s$  candidates invariant mass spectrum if we didn't take advantage of the particle identification of one of the kaons.

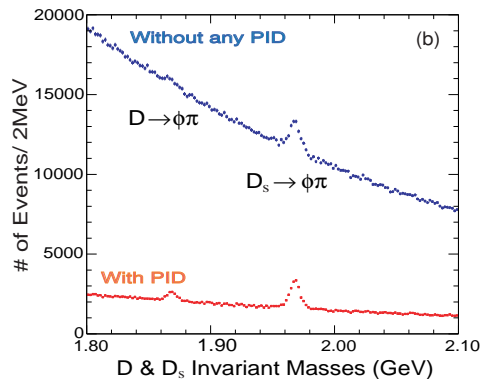


Fig. 7. The invariant mass of  $D$  and  $D_s$  candidates from the  $\Upsilon(4S)$  resonance data collected with the CLEO III detector without any PID (blue curve) and with RICH and  $dE/dx$  PID applied on just one of the kaons (red curve).

Table 2

Particle Identification efficiencies ( $\epsilon$ ) and fake rates (F.R) from CLEO III and CLEO-c data pions and kaons with momentum between 0.9 and 1.5 GeV/c and with a cut at 0 on the  $\chi^2$  difference between kaons and pions from a combined RICH and dE/dx information (the dE/dx doesn't have any significant separation ability in this momentum range). Errors here are statistical only.

Data type	Mom(GeV/c)	$\epsilon_\pi$ (%)	$K_{F.R}$ (%)	$\epsilon_K$ (%)	$\pi_{F.R}$ (%)
CLEO III	0.9	$96.8 \pm 1.7$	$2.3 \pm 0.8$	$91.8 \pm 1.6$	$0.8 \pm 0.4$
	1.1	$94.7 \pm 1.6$	$0.9 \pm 0.8$	$94.8 \pm 1.7$	$1.3 \pm 0.5$
	1.3	$95.7 \pm 1.5$	$4.6 \pm 0.6$	$91.7 \pm 1.6$	$1.8 \pm 0.5$
	1.5	$95.2 \pm 1.5$	$2.6 \pm 0.7$	$94.1 \pm 1.6$	$2.4 \pm 0.4$
CLEO-c	0.9	$95.1 \pm 2.1$	$5.9 \pm 2.9$	$87.2 \pm 3.6$	$0.8 \pm 1.3$

## 4 Conclusions

The CLEO LiF-TEA RICH is providing us with excellent particle identification for all momenta relevant to the CLEO III beauty threshold data and present charm threshold CLEOc data. It has operated successfully for over 4 years.

We have made and are making extensive studies of the Upsilon,  $B$  and  $B_s$  decays and, since last year, we have used the detector for the CLEO-c program to study charm mesons and charmonium decays. Thus, the physics performance of the CLEO RICH detector has met the benchmarks and the design criteria.

## 5 Acknowledgments

I gratefully acknowledge professors: S. Stone, M. Artuso, and T. Skwarnicki for the valuable discussions and comments and my CLEO collaborators especially G. Tatishvili for the

valuable input and N. Menea for the stimulating discussions. I would like also to thank the CESR staff for the excellent luminosity and the National Science Foundation for supporting this work.

## References

- [1] M. Artuso, Progress Towards CLEO III, in the Proceedings of the XXIX International Conference on High Energy Physics, Vancouver, Ed. by A. Astbury et al., World Scientific, Singapore, vol. 2, p 1552, [hep-ex/9811031] (1998).
- [2] A. Efimov and S. Stone, Nucl. Instr. and Meth. A371 (1996) 79.
- [3] M. Artuso *et al.*, Nucl. Instr. Meth. A441 (2000) 374-392.
- [4] M. Artuso *et al.*, Nucl. Instr. Meth. A502 (2003) 91-100.
- [5] D. Asner *et al.*, [CLEO Collaboration] ICHEP04-ABS11-0778 [arXiv:hep-ex/0408070], R. Sia [for CLEO collaboration] DPF 2004 [arXiv:hep-ex/0410087].